The Role of Non Quasi-Geostrophic Forcing During Cut-off Low Pressure System Onsets over South Africa

Tsholanang Solomon Rammopo and Thando Ndarana

13154402

HONOURS RESEARCH PROJECT REPORT – WKD763

2019

DEPARTMENT OF GEOGRAPHY, GEOINFORMATICS AND METEOROLOGY UNIVERSITY OF PRETORIA

ABSTRACT

The roles of non-quasigeostrophic forcing during three Cut-off low onsets over South Africa were elucidated using an extended quasigeostrophic height tendency equation at 500hPa. Advection terms reflected a cohesive pattern preceding the 10 March 2019 event onset which weakened thereafter when the advection of ageostrophic vorticity and the advection of absolute vorticity by the ageostrophic wind had opposing effects. The advection of geostrophic absolute vorticity contributed significantly towards height rises during CoL 2 formation with the advection of ageostrophic relative vorticity by the geostrophic wind playing a similar but secondary role. In addition, forcing time and area averages revealed that tilting and horizontal divergence consistently forced height rises and falls respectively. Poor forcing evolution average correlations between the respective diagnostic terms describing the three events were established while possible implications of the diagnostic results on medium-range forecasting scale predictability are discussed briefly based on the diagnostic terms' temporal signatures.

1. Introduction

Cut-off low-pressure systems (CoLs) can be described as closed low-pressure systems accompanied by a core of cold temperatures relative to the surrounding areas (Molekwa, 2013). They often bring about heavy rainfall and the possibility of floods over South African coastal areas, resulting in significant damage to property, infrastructure and the loss of life (Singleton & Reason, 2007; De Waal *et al*., 2017). The hazardous nature of the weather associated with CoLs (Favre, 2013; Engelbrecht, 2015) as well as the increased frequency of occurrence of such weather systems over South Africa (SA), (Favre, 2013) suggest that considerable efforts have to be devoted to the development of forecasting tools that may add value to the forecasting process of such weather systems.

In an attempt to address predictability problems associated with CoLs, the underlying dynamical processes associated with the onset of these systems need to be well investigated. Through the use of diagnostic equations, one can gain insight into the important aspects of the development of such extra-tropical systems as they unfold in a qualitative and mostly approximate manner to complement the Numerical Weather Prediction (NWP) guidance (Nielsen-Gammon & Gold, 2006). The quasigeostrophic (QG) theory (Bluestein, 1993; Holton & Hakim, 2012) diagnostics are often preferred in studies as opposed to finding solutions to the primitive equations due to its simplicity and ability to describe slow evolving synoptic waves in the mid-latitudes (Colucci & Dong, 2015) where the Rossby number is very small (Ro«1) and linear wave theory is assumed (Andrews *et al*., 1987; Gall, 1977). CoLs are essentially Rossby wave breaking (RWB) events (Ndarana & Waugh, 2010) which are non-linear processes (McIntyre & Palmer, 1985), as such it is important that any diagnostic intended to be used in the analysis of these systems must deviate from linear-wave theory. This is a requirement that the traditional QG diagnostics do not satisfy. Furthermore, there are several drawbacks of the QG framework which are attributable to the assumptions made in the formulation of the theory, effectively hampering its utility. These include; the assumption that the horizontal wind is purely geostrophic, thus ignoring ageostrophic processes, the exclusion of diabatic processes, and friction effects (Tsou *et al.*, 1987; Colucci & Dong, 2015), collectively referred to as non-quasigeostrophic (NQG) forcing.

Tsou *et al.* (1987) found that unlike the traditional QG height tendency equation, the extended form which takes into account diabatic effects, the ageostrophic components of the wind, and a three-dimensionally varying static stability parameter yielded a more realistic representation of an extratropical cyclone system. The results also revealed that the diabatic heating processes played an insignificant role in the development and maintenance of the intense extratropical cyclone. In addition, Colucci & Dong (2015) also derived an extended form of the QG height tendency equation (known as the non-quasigeostrophic (NQG) height tendency equation) which didn't take into account diabatic effects, but considered ageostrophic processes and a three-dimensionally varying static stability parameter like (Tsou *et al.*, 1987) which moderately improved the representation of physical mechanisms during Blocking onset.

Successful application of the extended QG height tendency in the analysis of a northern hemispheric extratropical cyclone together with the utility of the NQG tendency equation during the analysis of Blocking onset (which are also RWBs like CoLs (Ndarana & Waugh, 2010)) in the Southern Hemisphere (SH) suggests that for a more accurate analysis of CoL onsets over SA within the QG framework, an extended form of the chosen QG diagnostic has to be utilized. This is also due to the extratropical situation of SA and the non-linear nature of the systems. For this study, the NQG form of the height tendency equation (Colucci & Dong, 2015) which is briefly described in the following section, was the preferred diagnostic given how it retains the simplicity and usability QG diagnostics are known for. The choice was also supported by the insignificant role diabatic processes played during the development and maintenance of the extratropical cyclone studied by Tsou *et al.* (1987) which is totally ignored by the NQG diagnostic. In lieu of the above argument, it is reasonable to anticipate that the NQG diagnostic would be able to elucidate some of the key dynamical processes associated with CoL onset over South Africa with reasonable accuracy.

Potential to predict CoLs on the seasonal time scale exists (Engelbrecht, 2015) while the same can't be immediately said about the Medium Range Forecasting (MRF) scale. Furthermore, models such as the Global Forecasting Systems (GFS) can diverge when predicting CoLs due to the dynamic nature of the weather system (Lindsey, 2010). Lastly, the predictability of CoLs at the MRF scale is also limited by the fact that Ensemble Forecasting Systems (EFS) have no clear usable skill beyond 7 days (Tennant & Rae, 2007). The most basic approach of identifying CoLs in model output data is to identify the characteristic middle-upper air closed low-pressure coincident with a cold core described above. It is for this reason that a similar approach can be applied in forecast mode to determine the inception of such systems at various lead times within model forecasts.

The main objectives of this study were as follows; to diagnose CoLs over SA using an extended form of the QG height tendency equation, to assess the role of NQG forcing with particular interest on the ageostrophic wind related forcing during the onset of three CoLs as well as to establish and assess patterns relating to the terms in the NQG equation during the period preceding the onset of CoLs. These may inform aspects of predictability studies. The CoL events of interest were; the 10 August 2018, 10 March and 22 April 2019 events hereafter referred to as CoL1, 2 and 3 respectively.

2. Data and methods

Calculations were done using the 4x daily (6 hourly)re-analysis II dataset from the National Centre for Environmental Prediction (NCEP) with grid resolution of $2.5^\circ \times 2.5^\circ$ at 17 pressure levels (1000hPa-10hPa) for: air temperature, horizontal winds, geopotential height and vertical velocity (omega) fields. Attention was focused on the 500 hPa level due to the growth in QG calculated geopotential tendency errors at higher tropospheric levels and the stratosphere (Colucci & Dong, 2015).

As alluded to in the previous section, Eq. (1) (Colucci & Dong, 2015) was the chosen diagnostic on the basis of its consideration of ageostrophic processes and previous successful application in Southern Hemispheric (SH) Rossby Wave Breaking (RWB) studies such as blockings (which are associated with CoLs) (Colucci & Dong, 2015, Hoskins & Tyrlis, 2007, Ndarana & Waugh, 2010). In the derivation of this diagnostic, the total horizontal wind was used instead of the geostrophic wind while the static stability parameter was also allowed to vary three-dimensionally with height, unlike in the formulation of the traditional QG diagnostics. This is important because of the extra-tropical location of SA, where departures from pure geostrophy can be expected as well as the non-linear nature of CoLs.

$$
\begin{aligned}
\left[\nabla_p^2 + f_o^2 \frac{\partial}{\partial p}\left(\frac{1}{\sigma_p}\frac{\partial}{\partial p}\right)\right]\left(\frac{\partial z}{\partial t}\right) = & \overbrace{-\left(\frac{f_o}{g}\right)\mathbf{V_g}\cdot\nabla_p\left(\zeta_g + f\right)}^{\mathbf{F_{V1}}} \overbrace{-\left(\frac{f_o}{g}\right)\mathbf{V_g}\cdot\nabla_p\zeta_a}^{\mathbf{F_{V2}}} \overbrace{-\left(\frac{f_o}{g}\right)\mathbf{V_a}\cdot\nabla_p\left(\zeta + f\right)}^{\mathbf{F_{V3}}} \\
& \overbrace{-f_o^2\frac{\partial}{\partial p}\left[\left(\frac{1}{\sigma}\right)\mathbf{V_g}\cdot\nabla_p\left(\frac{\partial z}{\partial p}\right)\right]}^{\mathbf{F_{T1}}} \overbrace{-f_o^2\frac{\partial}{\partial p}\left[\left(\frac{1}{\sigma}\right)\mathbf{V_a}\cdot\nabla_p\left(\frac{\partial z}{\partial p}\right)\right]}^{\mathbf{F_{T2}}} \\
& \overbrace{-\left(\frac{f_o}{g}\right)\frac{\partial\zeta_a}{\partial t}}^{\mathbf{F_{ageo}}} \overbrace{-\left(\frac{f_o}{g}\right)\omega\frac{\partial\zeta}{\partial p}}^{\mathbf{F_{vert}}} \overbrace{-\left(\frac{f_o}{g}\right)\left(\zeta + f - f_o\right)\nabla_p\cdot\mathbf{V_h})}^{\mathbf{F_{div}}} \\
& \underbrace{}_{}\overbrace{-\left(\frac{f_o}{g}\right)\mathbf{k}\cdot\left(\nabla_p\omega\times\frac{\partial\mathbf{V_h}}{\partial p}\right)}^{\mathbf{F_{tilt}}}.
\end{aligned}
\tag{1}
$$

Basic variables such as ζ are as described in (Holton, 2004), while terms appearing in Eq. (1) are defined as follows:

- $\frac{\partial \mathbf{z}}{\partial \mathbf{t}}$: The geopotential height tendency,
- $\mathbf{F_{V1}}$: QG vorticity advection,
- $\mathbf{F_{V2}}$: Ageostrophic relative vorticity advection by the geostrophic wind
- $\mathbf{F_{V3}}$: Absolute vorticity due to the ageostrophic wind,
- $\mathbf{F_{T1}}$: QG thermal advection term,
- $\mathbf{F_{T2}}$: Thermal advection due to the ageostrophic wind,
- $\mathbf{F_{ageo}}$: Ageostrophic vorticity tendency,
- $\mathbf{F_{vert}}$: Vertical advection of relative vorticity,
- $\mathbf{F_{div}}$: Horizontal divergence term, and
- $\mathbf{F_{tilt}}$: Tilting term.

Onsets were defined as the first hour of the day (00Z) of CoL onset for each event. The onset day was defined as the day of the first occurrence of the cut-off closed low pressure, following (Molekwa, 2013).

The onset region was defined as the region completely enclosing the west flank of the cyclone spanning at least 20° latitudes and longitudes so as to include the area of maximum inward curvature characteristic of RWB to capture the behaviour of the terms during the evolution by calculating both area and time averages of the forcing terms during the evolution of each of the three CoLs. Onset regions (27.5° - 47.5° **S**;10° **W**-15° **E**), (25°-45° **S**;5° **W**-20° **E**) were defined for CoLs 1, 2, and 3 respectively (same region for CoLs 2 and 3).

All unknown variables appearing in Eq. (1) forcing terms were approximated numerically using finite differencing (central differentiation) in both the horizontal and verticals over 5 days prior and post-onset) with zero upper and lower boundary conditions for the pressure levels. Each forcing term was computed separately so as to isolate and assess its individual contribution (forcing) to $\frac{\partial \mathbf{z}}{\partial \mathbf{t}}$. This is warranted by the fact that for sinusoidal disturbances, the Laplacian of the function obtains a maximum value where the function is a minimum (Holton, 2004), resulting in Eq. (2). For purposes of visual interpretation, Eq. (2) was solved after calculations.

$$\left[\nabla_p^2 + f_o^2 \frac{\partial}{\partial p}\left(\frac{1}{\sigma_p}\frac{\partial}{\partial p}\right)\right]\left(\frac{\partial z}{\partial t}\right) \propto -\left(\frac{\partial z}{\partial t}\right). \tag{2}$$

A 9-point averaging filter was applied to each grid point to produce smooth results. Furthermore, extreme outliers, defined for this study as those points with values two orders of magnitudes higher than its eight surrounding members were removed and replaced by an interpolated value obtained by averaging eight neighboring points for each removed grid point.

The calculated area and time averages of the forcing terms were then used to produce time series plots for each CoL. A temporal low pass filter based on a fast Fourier transform (FFT) was applied to the evolution plots by removing fast-evolving processes at an interval of 6-12 hours for a cleaner depiction of the underlying evolution trends associated with the CoLs. To compare the association between the evolution of the three CoLs, each CoL time series was correlated linearly with the other two CoLs under investigation, for example, CoL 1 was correlated with CoL 2, then correlated with CoL 3 to produce three correlation coefficients.

3. Results

3.1 *NQG diagnostics*

Forcing for $\frac{\partial \mathbf{z}}{\partial \mathbf{t}}$ for the three CoL events were calculated and compared against one another. Generally, all the terms displayed fairly similar behavior during each of the three events, therefore only CoL 2 is extensively reported on. This is to avoid repetition, and due to the fact that CoL 2 has properties relating to both CoL 1 and CoL 2, e.g CoL 1 propagated zonally at a fairly consistent rate, while CoL 3 was quasi-stationary for some time after onset, while CoL 2 moved relatively slower as compared to CoL 1, but at an increased speed relative to CoL 3. Therefore CoL 2 is considered as the average of the CoLs in this study.

Table. 1 reveals that Fv1 was on average the most significant forcing term two days prior the three CoLs' onsets with a value of 0.8755 $\times$ 10^3 m$\times$ $6h^{-1}$ as previously found by other studies (Tsou *et al.*, 1987; Colucci & Dong, 2015). It is worth noting that FT1's contribution was more variable than its QG associated Fv1 between the different events, an expected observation given that it was anticipated that FT1 is more prominent at lower levels of the atmosphere. This potentially reveals a difference in behavior and dynamical processes between two classes of CoLs, those that remain quasi-stationary for a prolonged period of time (CoL 3), and those that propagate continuously (CoLs 1 and 2). FT1 contributes significantly towards height falls (negative values) for quasi-stationary types in contrast with the mobile type which have FT1 as a contributor towards height rises (positive values).

Table. 1: Area averages of all forcing terms averaged over a 48 hour pre-onset period, units: $\times 10^3\ m\times 6h^{-1}$

Forcing Term	**CoL 1**	**CoL 2**	**CoL 3**	**Average**
Fv1	1.0563	0.6155	0.9547	0.8755
Fv2	0.517	0.4039	0.3496	0.4235
Fv3	0.2697	0.422	0.3697	0.3538
FT1	0.2295	0.5961	-0.4517	0.124633
FT2	-0.6607	-0.3754	0.0219	-0.33807
Fageo	-0.1246	-0.0991	-0.1	-0.1079
Fvert	-0.5934	-0.6677	-0.2754	-0.51217
Fdiv	-0.1428	-0.2235	0.0064	-0.11997
Ftilt	0.4336	0.4734	0.1769	0.3613
Height Tendency	2.5531	2.2458	3.66	2.819633

While the terms appearing on the right-hand side (RHS) of Eq. 1 are forcing terms, we can infer from their magnitudes, the relative contributions of different physical mechanisms to the geopotential height tendencies represented by these terms. Prior to CoL 2 onset, terms: Fv1, Fv2, Fv3, FT1 and FT2 acted in cohesion as the mechanisms responsible for the northeastward propagation (Fv1, Fv2 and Fv3) and intensification (FT1 and FT2) of the trough-ridge system through cold cyclonic advection to the left (west) of the trough and warm anticyclonic vorticity advection on the right of the trough associated with height rises and falls respectively. This is due to the collocation of vorticity terms'(Fv1, Fv2, and Fv3) maxima and minima with the trough-ridge axes which implies that vorticity does not contribute towards the intensification, therefore suggesting that it is responsible for system motion. Furthermore, zero thermal advection (FT1 and FT2) along the trough-ridge axes is associated with the intensification of the system (Holton, 2004).

Most notable of the NQG forcing is Fvert's persistent forcing towards height falls over the onset region 48 hours prior to onset followed by FT2 on average for the three cases (Table. 1). In contrast, Fv2 was the leading positive term, persistently forcing height rises followed by Ftilt while FT2 and Fdiv contributed negligibly towards height rises. The advection of ageostrophic relative vorticity by the geostrophic and the advection of absolute vorticity by the ageostrophic wind were the most significant NQG processes inducing geopotential height rises over the onset region prior to the CoLs' onsets while the thermal advection by the ageostrophic wind and the vertical advection of relative vorticity were the NQG processes most responsible for the height falls within the onset regions.

The temporal and spatial evolution of the four significant contributing terms 48 hours prior to CoL 2 onset can be seen in Figures 1. (a-d). Figure. 1(a) reveals that Fv1 decreases in intensity between 6 and 9 March followed by a moderate increase in positive values between 9 and 10 March (Onset day) as suggested by Table. 1 followed by an alternating contribution during subsequent days after the onset as the CoL matures and decays. A similar pattern is observed for Fv2 (Fig. 1(b)) while FT2 and Fvert (Fig. 1(c) and 1(d) respectively) show a peak in negative values prior and during onset, while it is also observed that Fvert predominantly contributes towards height falls during most days preceding the onset.

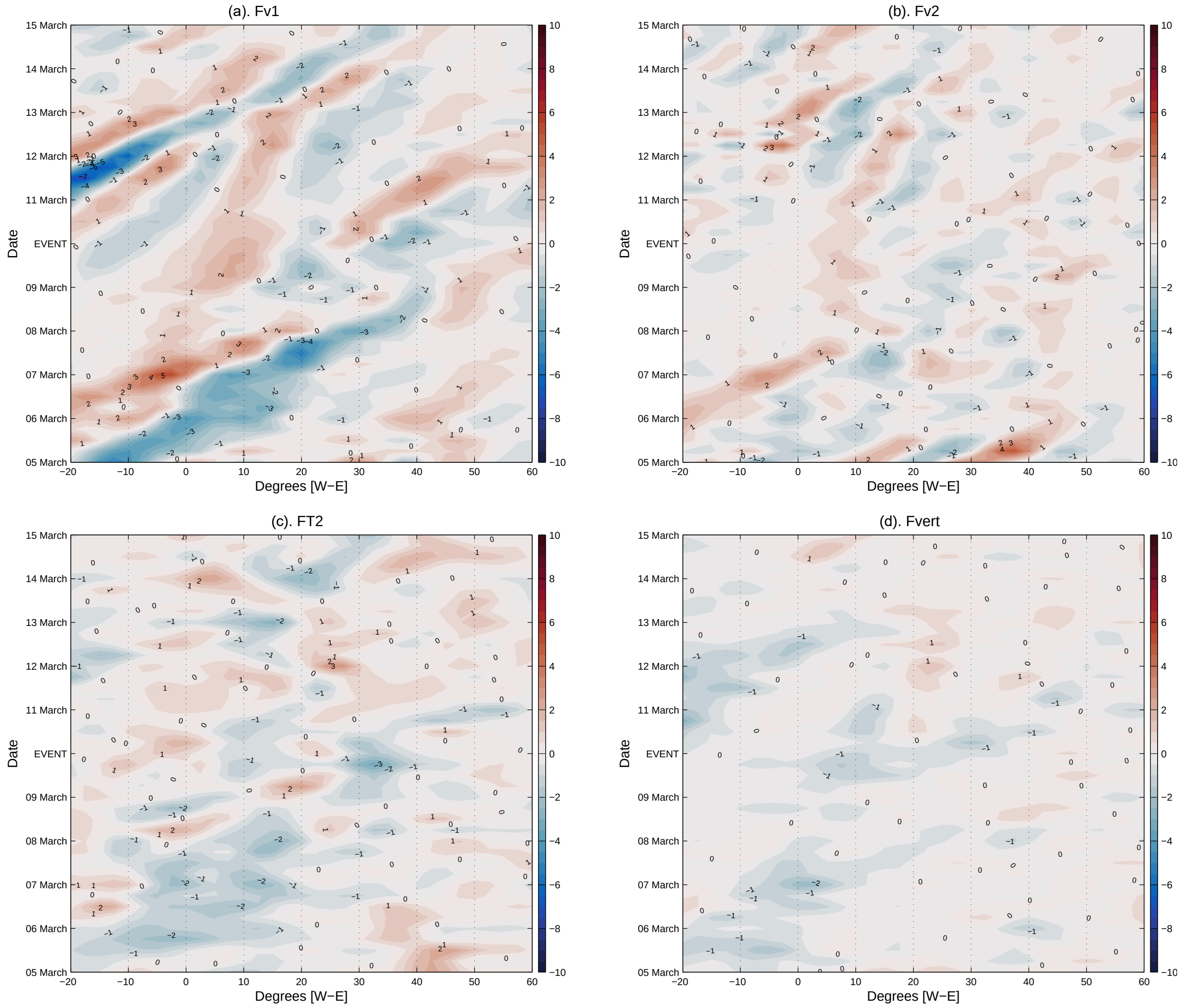

Figure. 1(a): Hövmöller diagram showing the evolution of (a). Fv1, (b). Fv2, (c). FT2 and (d). Fvert during and after CoL 2 averaged over region (20° *-* 40° **S***), units:* $\times\, 10^3$ *m*$\times\, 6h^{-1}$*.)*

After onset, the contributions of the terms are less clearly defined. The contributions of the terms, particularly those resulting from the inclusion of the ageostrophic wind depict different behaviors around the closed low pressure (geopotential heights) in contrast with their initial behavior prior to onset, suggesting that NQG terms and processes played a complementary role to the QG processes as the CoL 2 matured. Fig 2(a) and (b) show the complement of Fv2 and Fv3 24 hours after onset, having the net effect of neutralizing the geopotential height tendencies over the matured CoL 2 as seen in Fig. 2 (d) of which 24 hours earlier during onset Fig. 2(c) pronounced height rises were observed over the west flank of the closed low pressure coupled with dropping heights on the east flank. A comparison of Figs. 2(a-d) reveals that Fv2 had a bigger contribution towards height tendencies as areas of positive and negative values in Fig. 2(a) coincide with areas of rising and falling geopotential heights (Fig. 2(d)) respectively. A similar complement pattern observed for Fv2 and Fv3 was observed for FT1 and FT2 (not shown).

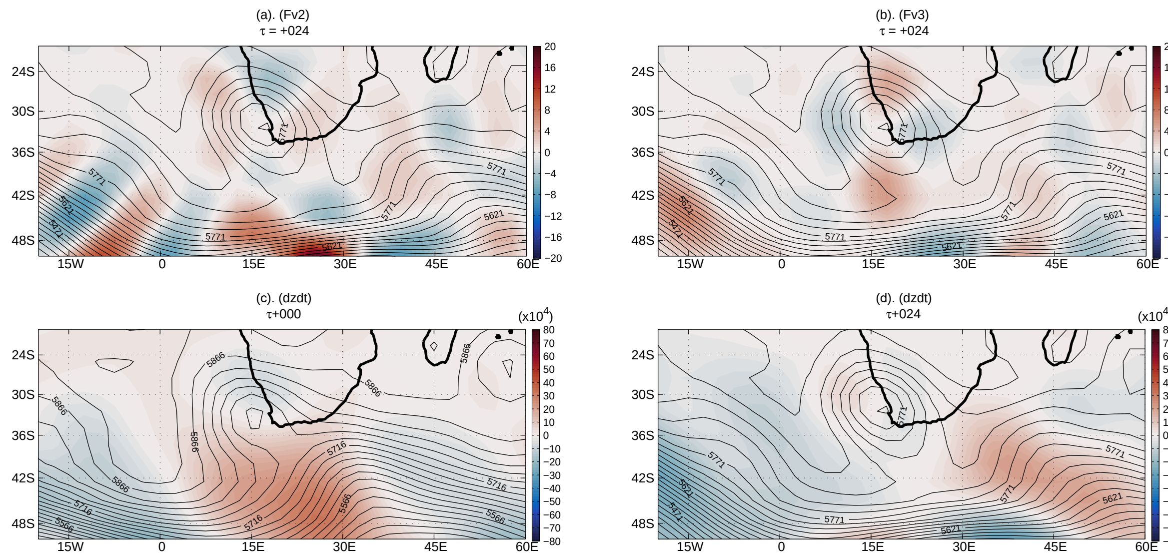

Figure. 2: 500 hPa geopotential heights(black contours) overlaid with Fv2 (a) and Fv3 (b) 24 hours post CoL 2 onset at 00Z and height tendecies during (c) and 24 hours (d) after onset , units: $\times\ 10^3\ m\times\ 6h^{-1}$

3.2 *COL evolution trends*

Figure 3 depicts the 10-day time series of Fv3 over CoL 2 onset region as well as over a region (25° - 35° **S**; 7.5° **W** - 7.5° **E**) where a CoL could have developed, but the low failed to cut-off from the main flow on 8 March 2019, 00Z. It is clear that an evolution pattern depicting CoL 2 is distinct from that of a trough that portrayed similar characteristics to those of the onset of a CoL. This suggests that CoLs may have distinct temporal signatures in terms of NQG terms that may be utilized to diagnose the presence of CoLs and the possibility of their occurrence based on a trend analysis of the NQG term forecasts. Figures. 4(a-d) are examples of some of the distinct temporal signatures produced by the NQG terms (Fv2, Fv3, FT2, and Fvert) before and after onset for the three analyzed cases.

It is evident that the trends are similar for the most part between the different CoLs, with the most notable differences are seen with CoL 3, a quasi-stationary type of CoL as described in previous sections. Furthermore, while the shapes of the trends are generally similar, the timings of the different portions of the trends are different, e.g in Fig. 4(a), Fv2 ”dips” a day later for CoL 3 than for CoLs 1 and 2 between two days before and during onset, therefore, such lack of synchronicity between the patterns is seen by low correlation values in Table. 2 and hence contributed negatively to the linear correlation regardless of the similarities between the shapes.

One of the most basic ways of diagnosing CoLs is to look for a closed low-pressure centre coinciding with a core of low pressure as alluded to in the introductory section. This suggests that the predictability of CoLs on the medium-range forecasting scale (MRF) relies on a very limited number of variables, e.g geopotential heights, temperature, and wind. It is known that no Numerical Weather Prediction (NWP) model will produce consistently accurate forecasts of the basic atmospheric variables (Dyson & Van Heerden, 2002), therefore it is important to consider an assortment of variables and terms to account for the inevitable uncertainty related to both ensemble prediction systems (EPS) and deterministic models. The observed temporal signatures in Fig. 4(a-d) suggest that CoLs may have signatures that could possibly act as an indication of a possible development of a CoL at specified lead times. The above findings further suggest that the predictability of such patterns is an aspect that could be further investigated as part of MRF predictability studies of rain and severe weather producing weather systems over South Africa.

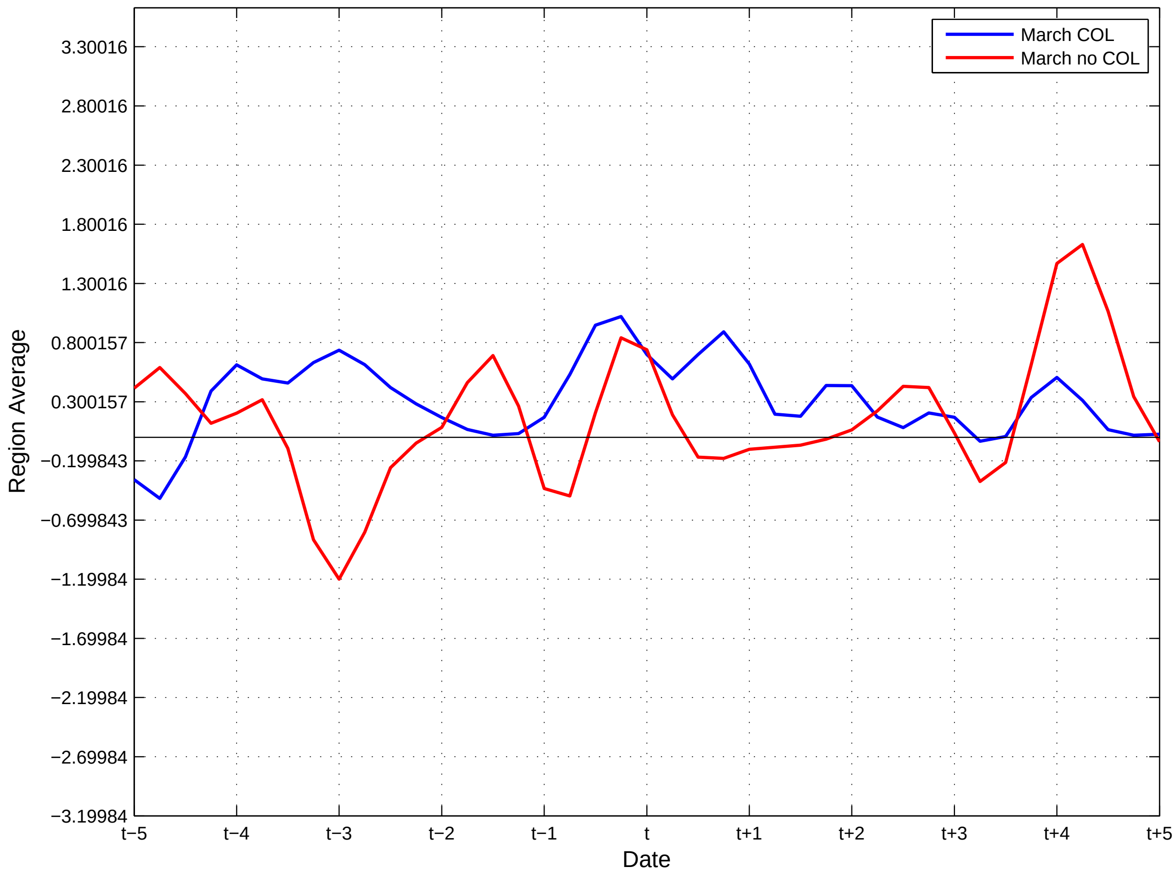

Figure. 3: A comparison of the evolution of Fv3 over a 10-day pre- and post-onset period over the CoL 2 onset region and a region (25° - 35° **S***;* 7.5° **W** - 7.5° **E***) yielding no CoL.*

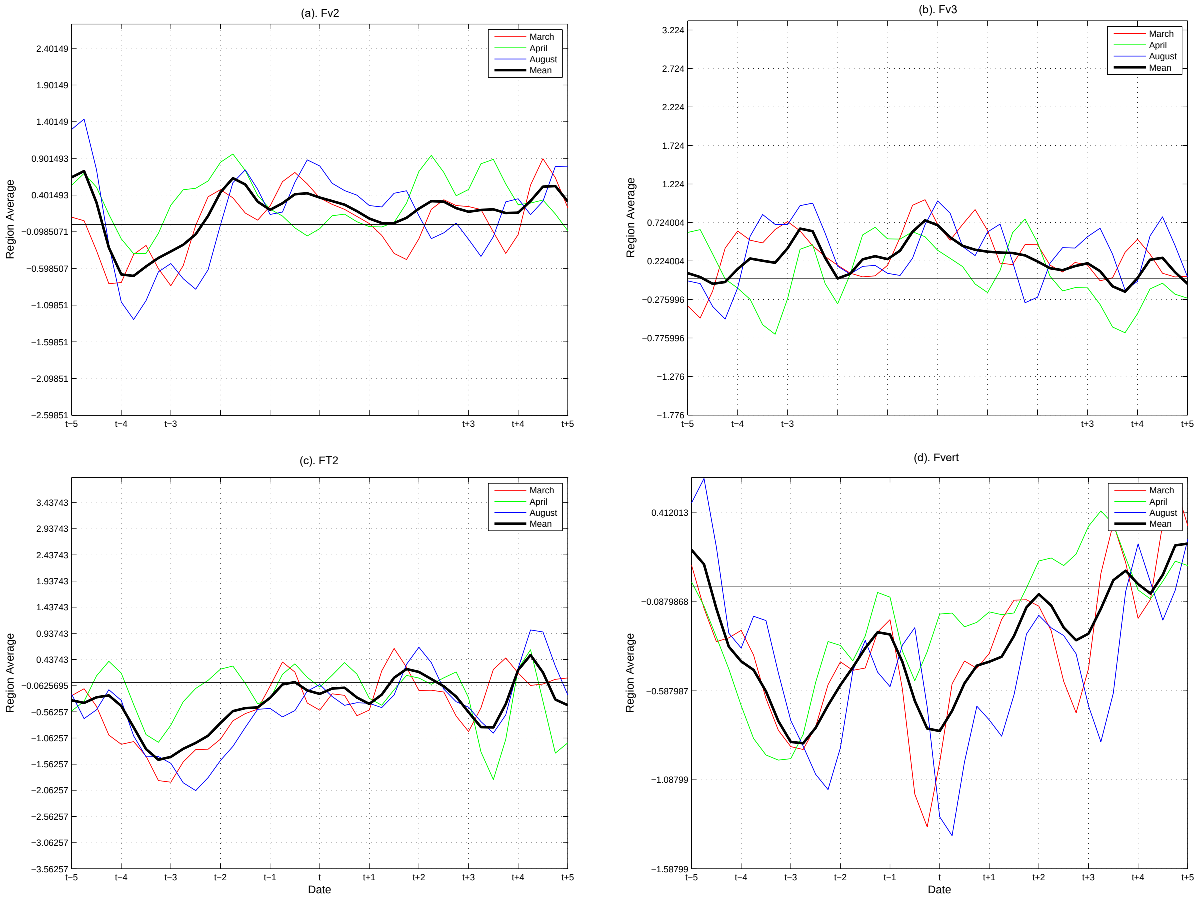

Figure. 4: A comparison of the evolution of (a). Fv2, (b). Fv3, (c). FT2 and (d). Fvert over the 10-day pre- and post onset period between the three CoLs.

Table. 2: Correlations (CoL1 and CoL2, CoL2 and CoL 3, etc) of the evolution of forcing terms during the 5-day pre-onset period.

Forcing Term	CoL 1+2	CoL 1+3	CoL 2+3	Mean
Fv1	0.7886	0.9602	0.7839	0.8442
Fv2	0.3217	0.1634	0.0548	0.1800
Fv3	0.3449	0.7528	0.4025	0.5001
FT1	0.1577	0.7033	0.0069	0.2893
FT2	-0.0928	0.3781	-0.0824	0.0676
Fageo	0.2333	0.1108	0.2797	0.2079
Fvert	0.0399	0.1084	-0.5466	-0.1327
Fdiv	0.0721	-0.1351	-0.2728	-0.1119
Ftilt	-0.1710	-0.2371	0.4216	0.0045

4. Conclusion

Three CoL events were diagnosed over SA using an extended form of the QG geopotential height tendency equation (Colucci & Dong, 2015) in line with the objectives of this study. Consistent with previous studies, it is found that for the analyzed CoLs, QG advection processes (Fv1) dominate trough-ridge development while NQG terms play occasional secondary roles (Godoy *et al*., 2011). NQG equivalents assumed a complementary role to have a net influence on $\frac{\partial z}{\partial t}$. The roles of NQG unrelated to advection were also analyzed. Fvert and Ftilt contributed on average significantly towards height falls and rises over time within the onset region. An evolution pattern of the forcing terms was established and found to be approximately consistent throughout the three CoLs which then begs the question, how useful could the pattern be for predictability studies of weather systems on the MRF scale? The findings of the study serve as testament that there is some knowledge to be gained about the dynamical processes governing the life cycles of rain-bearing weather systems over South Africa from the utility of simple, traditional diagnostics in for the purposes of research.

8. References

Andrews, D. G., Leovy, C. B., & Holton, J. R. (1987). *Middle atmosphere dynamics* (Vol. 40). Academic press.

Bluestein, H. B. (1993). *Synoptic-dynamic meteorology in midlatitudes. volume ii. observations and theory of weather systems*. New York, NY (United States); Oxford University Press.

De Waal, J. H., Chapman, A., & Kemp, J. (2017). Extreme 1-day rainfall distributions: Analysing change in the western cape. *South African Journal of Science*, *113*(7-8), 1–8.

Dong, L., & Colucci, S. J. (2015). The role of nonquasigeostrophic forcing in southern hemisphere blocking onsets. *Monthly Weather Review*, *143*(4), 1455–1471.

Dyson, L., & Van Heerden, J. (2002). A model for the identification of tropical weather systems over south africa. *Water SA*, *28*(3), 249–258.

Engelbrecht, C. J., Landman, W. A., Engelbrecht, F. A., & Malherbe, J. (2015). A synoptic decomposition of rainfall over the cape south coast of south africa. *Climate Dynamics*, *44*(9-10), 2589–2607.

Favre, A., Hewitson, B., Lennard, C., Cerezo-Mota, R., & Tadross, M. (2013). Cut-off lows in the south africa region and their contribution to precipitation. *Climate dynamics*, *41*(9-10), 2331–2351.

Gall, R. (1977). Some non-quasigeostrophic effects in linear baroclinic waves. *Monthly Weather Review*, *105*(8), 1039–1051.

Godoy, A. A., Possia, N. E., Campetella, C. M., & García Skabar, Y. (2011). A cut-off low in southern south america: Dynamic and thermodynamic processes. *Revista Brasileira de Meteorologia*, *26*(4), 503–514.

Holton, J. R., & Hakim, G. (2004). *An introduction to dynamic meteorology* (Vol. 41) (No. 5). AAPT.

John, L. (2010). *Cut-off lows are highly unpredictable.* Retrieved from `https://www.sanluisobispo.com/news/weather/weather-watch/article39123609.html`

McIntyre, M., & Palmer, T. (1985). A note on the general concept of wave breaking for rossby and gravity waves. *pure and applied geophysics*, *123*(6), 964–975.

Molekwa, S. (2013). *Cut-off lows over south africa and their contribution to the total rainfall of the eastern cape province* (Unpublished doctoral dissertation). University of Pretoria.

Ndarana, T., & Waugh, D. W. (2010). The link between cut-off lows and rossby wave breaking in the southern hemisphere. *Quarterly Journal of the Royal Meteorological Society*, *136*(649), 869–885.

Singleton, A., & Reason, C. (2007). A numerical model study of an intense cutoff low pressure system over south africa. *Monthly weather review*, *135*(3), 1128–1150.

Tennant, W. J., Toth, Z., & Rae, K. J. (2007). Application of the ncep ensemble prediction system to medium-range forecasting in south africa: New products, benefits, and challenges. *Weather and forecasting*, *22*(1), 18–35.

Tsou, C. H., Smith, P. J., & Pauley, P. M. (1987). A comparison of adiabatic and diabatic forcing in an intense extratropical cyclone system. *Monthly weather review*, *115*(4), 763-786.